http://ijopaar.com; 2016 Vol. 3(2); pp. 146-152

Lattice Boltzmann Method for PAKKA-Model Structures in Fluid Flow Motion

Dr. Mohammad Miyan

Associate Professor, Department of Mathematics,
Shia P. G. College, University of Lucknow,
Lucknow, India-226020.
Email: miyanmohd@rediffmail.com

Date of revised paper submission: 22th August 2016; Date of acceptance: 12st September 2016
Date of publication: 30th September 2016; Impact Factor: 3.498; Quality Factor: 4.39
***First Author / Corresponding Author; Paper ID: A16308**

Abstract

In the Lattice Boltzmann method particles are generally allowed to move and collide on the lattice. The rules governing the collisions are designed in such a way that the time-average motion of the particles is consistent with the Navier-Stokes equations. The Lattice Boltzman method has multiple the advantages as its time and space efficient calculations are forwarded to parallelize, it handles the complex boundaries without any difficulty and it directly links the microscopic and the macroscopic phenomena.

By the Lattice Boltzmann simulations there are the examination of quality of the numerical models of the porous media and tomographic imaging techniques. The different models were taken to give the qualitatively dependence of permeability on porosity, but it also effects of other structural properties were shown. These include specific surface area, tortuosity, shape and orientation of particles in the medium. The transverse and in-plane flow simulations for PAKKA-model samples augmented the characteristics of samples and the solutions e.g., effect of the fibre flexibility. The simulations show that results on paper can be sensitive to imaging techniques, since the differences in permeability between high and low-resolution images can be seen though results within each technique were consistent. The graphs and table indicate the dependency and variation of porosity on Darcy permeability and tortuosity.

Keywords: Lattice-Boltzman method, Multiphase flow, PAKKA-model structure.

1. Introduction

In the theory of fluid mechanics for the three dimensional images, the fluids are represented with volume and iso-surfaces visualization techniques by using intensity, color and transparency for denoting the fluid density. The fluid movement is observed by the assembling visualizations at the series of various time steps into animations. The three dimensional images also use iso-surfaces to delineate the structure of the medium or the surface of structure in which the fluid flow is to be modeled.

The paper related of the fines, fibres, fillers and some other additives that are configured in the complex, spatial solid materials formed in the paper formation process. We know that porous structure is given explicitly when fibre network is given and the term paper structure will be taken as the common structure. The paper structure gives actual paper properties indirectly or directly together with material properties of solid materials. The three-dimensional paper structure is much important phenomenon for paper material; it is very important to know the detailed knowledge of it. But it is the difficult task as the three-dimensional structure is by nature hard to access. The indirect methods have been applied for characteristic features of the paper structure. Now, only such indirect methods have been used for characterizing the structure of the paper. The x-ray and microscopy techniques and increased computer capacity allow the procedures for the development of the whole three-

dimensional paper structure. The methods give the development of the knowledge on paper structure and how it affects the macroscopic analysis of the paper properties. So that methods to explore how three-dimensional paper structure is related to macroscopic paper properties are now emerging, alternative indirect methods have been applied for the decades of years. The well expertise papermakers know how to varying the production settings for improving certain paper characteristics and then to change the structure of paper [4], [5].

2. Method and Equations

The motion of fluid is given by the basic equation of fluid mechanics, i.e., the equation of continuity given as

$$\frac{\partial \rho}{\partial t} + \nabla.(\rho\, u) = 0 \tag{1}$$

The Lattice Boltzman method was properly observed and the equations were derived by Aaltosalmi, U., et al. [1], [2], [3]. The Lattice-Boltzman hydrodynamics is the mesoscopic approach for computational fluid mechanics. The system of macroscopic dynamics will be shown for satisfying the Navier-Stokes equation. In the present paper, there is analysis of the fluid and is modeled by the particle distributions which moves on lattice divided to various fluid particles. In the concept of one lattice time period, the particles propagate with their adjacent lattice points and distribute the momentum in collision. The density and velocity of entering particle at site r and time t in some arbitrary directions c_i can be written as the equation (2).

On taking $f_i(r, t)$ the particle density entering at the site r and at time t with the velocity pointing in the direction c_i, where i shows the lattice directions. For the lattice time step η and lattice spacing λ, the particle velocities are given as:

$$v_i = \frac{\lambda}{\eta} c_i \tag{2}$$

The evolution equation for f_i is given as:

$$f_i(r + \lambda c_i, t + \eta) = f_i(r, t) + \omega_i(r, t) \tag{3}$$

Where $\omega_i(r, t)$ is a collision term i.e., model dependent and decreases or increases the density of type i particles. As similar to the kinetic theory, the quantities i.e., density ρ, velocity v and momentum tensor M are shown by the equations

$$\rho(r, t) = \sum_{i=1}^{n} f_i(r, t) \tag{4}$$

$$\rho(r, t) v(r, t) = \sum_{i=1}^{n} v_i\, f_i(r, t) \tag{5}$$

$$M_{jk}\,(r, t) = \sum_{i=1}^{n} v_{i\alpha}\; v_{i\beta}\; f_i(r, t) \tag{6}$$

Where the suffix j and k are spatial components of velocity vectors and n shows the number of possible directions c_i. In the lattice Boltzman dynamics, we have

$$M_i = \frac{1}{\xi}\left(f_i^{(0)}(r, t) - f_i(r, t)\right) \tag{7}$$

which is based on the single collision relaxation. Then the evolution equation for the system can be taken as:

$$f_i(r + \lambda c_i, t + \eta) = f_i(r, t) + \frac{1}{\xi}\left(f_i^{(0)}(r, t) - f_i(r, t)\right) \tag{8}$$

Here ξ is relaxation parameter. The term shown in equation $f_i^{(0)}$ is the equilibrium distribution as taken to give the required behavior of fluid.

The expansion of equation (8) by the Taylor's method on retaining the term up to second order and neglecting the higher order terms, we have

$$\eta \frac{\partial}{\partial t} f_i + \lambda (c_i . \nabla) f_i + \frac{\eta^2}{2} \frac{\partial^2}{\partial t^2} f_i + \frac{\lambda^2}{2} (c_i . \nabla)^2 f_i + \lambda \eta (c_i . \nabla) \frac{\partial}{\partial t} f_i = \omega_i \quad (9)$$

$$f_i = f_i^{(0)} + \varepsilon f_i^{(1)} + \varepsilon^2 f_i^{(2)} + \cdots + \varepsilon^n f_i^{(n)} + \cdots \quad (10)$$

Here ε is small parameter. For finding the term $f_i^{(n)}$, n = 0, 1, 2,.., we have

$$\rho = \sum_{i=1}^{n} f_i^{(0)}, \rho\, v = \sum_{i=1}^{n} v_i\, f_i^{(0)} \quad (11)$$

$$\sum_{i=1}^{n} f_i^{(n)} = 0, \qquad \sum_{i=1}^{n} v_i\, f_i^{(n)} = 0\,; n \geq 1 \quad (12)$$

Taking

$$\frac{\eta}{t_1} = o(\varepsilon),\ \frac{\eta}{t_2} = o(\varepsilon^2) \quad (13)$$

Where t_1 and t_2 are macroscopic time scales.

Also,

$$\frac{\lambda}{L_1} = o(\varepsilon) \quad (14)$$

Also by cosidering,

$$\frac{t_1}{\varepsilon} + \frac{t_2}{\varepsilon^2} = t, r = \frac{r_1}{\varepsilon} \quad (15)$$

Where r_1 is the macroscopic scale variable. We have

$$\frac{\partial}{\partial t} = \varepsilon \frac{\partial}{\partial t_1} + \varepsilon^2 \frac{\partial}{\partial t_2} \quad (16)$$

$$\frac{\partial}{\partial j} = \varepsilon \frac{\partial}{\partial (1j)} \quad (17)$$

Now all the velocities do not have the same mass m_i, so we can write

$$\sum_{i=1}^{n} m_i c_{ij} = 0 \quad (18)$$

Let us take the function $f_i^{(0)}$ as function of quantities ρ and ρu, we have

$$f_i^{(0)} = m_i F_i^{(0)}$$

$$f_i^{(0)} \cong m_i \left(a_1 \rho + \frac{a_2}{v^2} \rho\, v_i . u + \frac{a_3}{v^2} \rho \frac{u^2}{v^2} + \frac{a_4}{v^4} \rho\ (v_i . u)^2 \right) \quad (19)$$

Here a_1, a_2, a_3 and a_4 are taken as arbitrary constants. The collision operator ω_i will conserve mass and momentum, so we have

$$\sum_i \omega_i = 0, \sum_i \omega_i\, v_i = 0 \quad (20)$$

The derivation of Navier-Stokes equation by expanding the Boltzman equations (13), (14) and (20), [3] we get

$$\frac{\partial \rho u_j}{\partial t} + \frac{\partial}{\partial k}\left[M_{jk} + \frac{\eta}{2}\left(\varepsilon \frac{\partial}{\partial t_1} M_{jk}{}^{(0)} + \frac{\partial}{\partial l}\left(\sum_i m_i \, v_{ij} v_{ik} v_{il} \, F_i{}^{(0)} \right) \right) \right] = 0 \qquad (21)$$

The momentum tensor M_{jk} [3] can be determined by

$$M_{jk} = M_{jk}{}^{(0)} + M_{jk}{}^{(1)} + M_{jk}{}^{(2)} + \cdots \qquad (22)$$

$$F_i{}^{(1)} = -\eta\varepsilon \frac{a_2}{v^2}\left(v_{ij} v_{ik} - \frac{a_1 v^2}{a_2}\delta_{jk} \right) \frac{\partial}{\partial(1j)} (\rho \, u_k) \qquad (23)$$

3. Numerical Simulations and Figures

For the PAKKA-model Structure, the fibre webs are grown randomly depositing flexible fibres having the rectangular cross section on left substrate. These are the periodic in *xy*-plane. For making structures homogeneous, surface layers perpendiculars to z-axis are removed. The porosity of sample is organized by varying the flexibility of fibres. In this model, fibre width to length ratio is 1/20 and the sample size is four fibre lengths in *xy*-plane and ten fibre width in *z*-direction. For determination of anisotropy of permeability, the imposed boundary conditions are selected in such a way to use the structural symmetry inherent in model. The different sample models [1], [2], [3] are shown in the figures-1, 2 and 3.

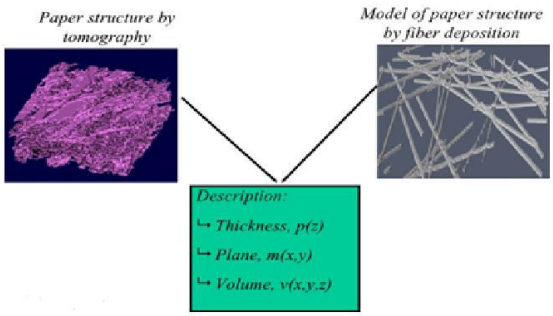

Figure-3.1

(Generalized description of the three dimensional structure of paper sample [14])

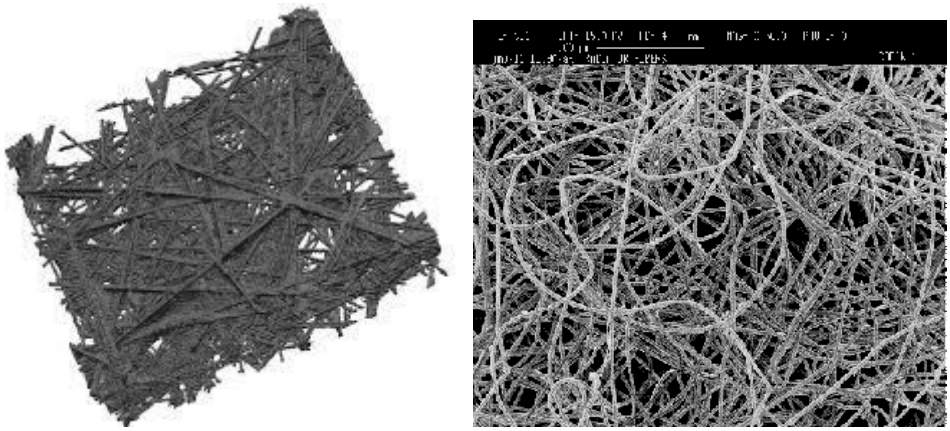

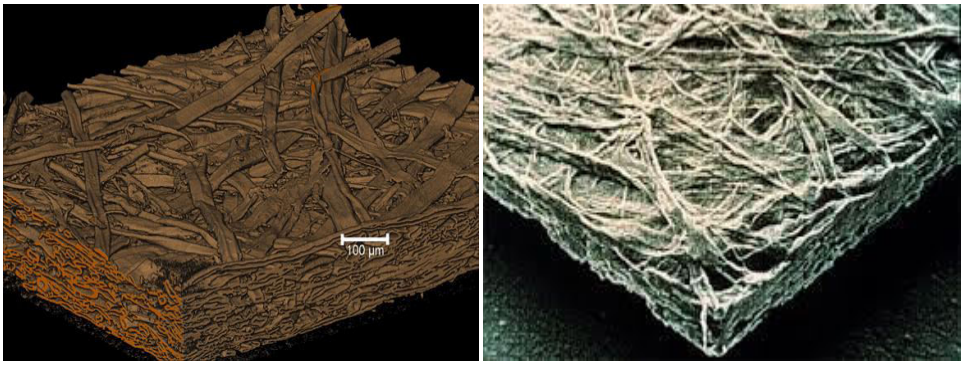

Figure-2

(Some PAKKA-model samples)

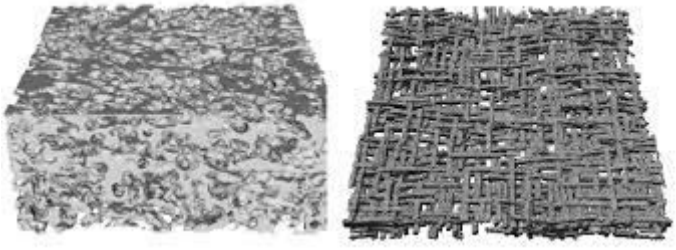

Figure-3

(PAKKA-model sample: A sample with fines and randomly oriented fibres [3])

For the transverse flow, the fluid layers of not less than 0.1% of the thickness of the sample are added up and down side of sample. The periodic boundary conditions are used in the *z*-direction and also in the *xy*-plane due to periodicity of the PAKKA-model in these directions. For in plane flow, frictionless slip conditions are imposed at boundaries perpendicular to the *z*-direction. The values calculated by various experiments are shown in the table-2.1 [3], [6], [7], [8].

Table-1. (The structured parameters and simulated quantities the four different samples)

Sample	*T (mm)* *Thickness*	ϕ *Porosity*	*k* (10^{-10} m^2) *Darcy permeability*	*S* (10^3 / *m*) *Pore surface area per volume of sample*	τ *Tortuosity*
A	0.58	0.479	0.510	20.2	1.190
B	0.87	0.526	1.47	16.6	1.171
C	0.66	0.530	0.937	20.5	1.174
D	0.87	0.560	0.61	15.4	1.166

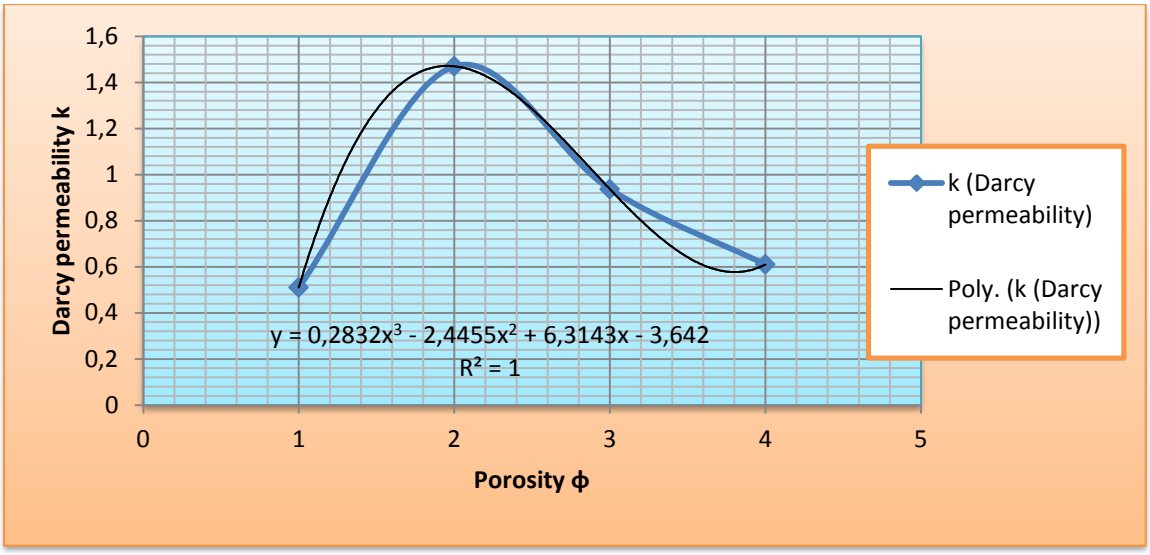

Figure-5 (Variation of Darcy permeability k with porosity ϕ with third order polynomial variation trendline curve) $y = 0.283\ x^3 - 2.445\ x^2 + 6.314\ x - 3.642$

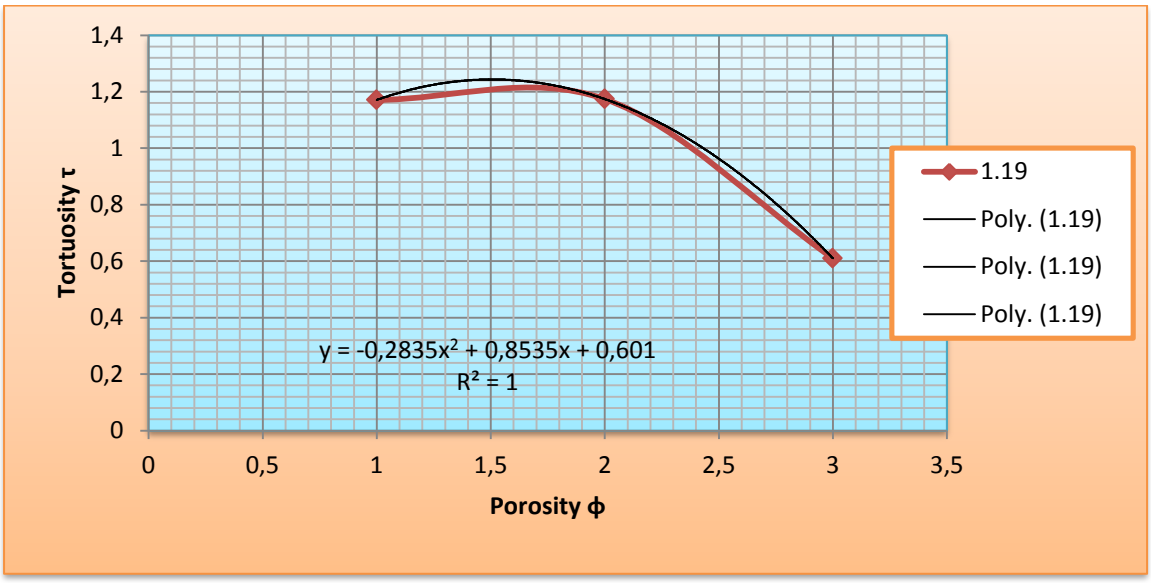

Figure-6 (Variation of Tortuosity τ with porosity ϕ with third order polynomial variation trendline curve)

4. Conclusion

The lattice-Boltzmann method is used for solve 3-D Newtonian fluid-flow problems in the porous media given by tomographic imaging and by the numerical modelling. By lattice-Boltzmann simulations there are the examination of quality of numerical models of the porous media and the tomographic imaging techniques. The different models were taken to give the qualitatively dependence of permeability on porosity, but also effects of various structural properties were demonstrated. These include specific tortuosity, surface area, shape and orientation of particles in medium. The transverse and in-plane flow simulations for the PAKKA-model samples augmented characteristics of the samples and give e.g. the effect of the fibre flexibility. The simulations show that the results on paper can be sensitive to the imaging processes, since permeability differences between low and high-resolution images will be seen since the results within each process were consistent. The third order polynomial variations of porosity ϕ with respect to Darcy's permeability k and Totuosity τ are shown by equations (24) and (25) respectively.

$$y = 0.283\ x^3 - 2.445\ x^2 + 6.314\ x - 3.642 \quad (24)$$

$$y = -\ 0.283\ x^2 + 0.853\ x + 0.601 \quad (25)$$

The table and graphs analyze the variation and dependency of porosity on Darcy permeability and tortuosity.

Hence the results obtained show that fluid-flow simulations for the PAKKA-model samples and tomographic images of the paper grades, can produce results that are similar to those found in the experiments. There are obviously also the experimental factors, such as e.g. swelling of fibres in the water, which are not included in the present simulations. The fluid flow simulation results of the various paper grades could increase the reliability of modelling the processes of paper making, and those of wires the possibilities for examine and develop the paper machine clothing.

References

1. Aaltosalmi, U., et al., "Numerical analysis of fluid flow through fibrous porous materials", International Paper Physics Conference, Proceedings, (2003), pp. 247-252.
2. Aaltosalmi, U., et al., "Numerical analysis of fluid flow through fibrous porous materials", JPPS 30 (9) (2004) 251–255.
3. Aaltosalmi U., "Fluid flow in porous media with the Lattice-Boltzmann method", University of Jyväskylä, *Research report No*. 3/2005Finland, (2005): pp.39-45.
4. Holmstad, Rune, et al., "Modelling the paper sheet structure according to the equivalent pore concept", *Proceedings from the Cost Action E11–Characterisation methods for fibres and paper* 15 (2001): 25.
5. Holmstad, Rune, et al., "Quantification of the three-dimensional paper structure: Methods and potential", *Pulp and Paper Canada* 104.7 (2003): 47-50.
6. MANWART, C., et al., "Lattice-Boltzmann and finite difference simulations for the permeability of three-dimensional porous media", Phys. Rev. E 66, (2002) 016702.
7. Miyan, M., "The Two Phase Flow Motions and their P. D. F. Representations", *International Journal of Pure and Applied Researches (IJOPAAR),* (2016), Volume 1(Issue 1), pp. 31-39. http://ijopaar.com/files/CurrentIssue/A16105.pdf
8. Miyan, M., "Load Capacity for Fitted Bearings of Hydrodynamic Lubrication under Low and High Rotation Number", *International Journal of Pure and Applied Researches (IJOPAAR),* (2016), Volume 1(Issue 2), pp. 109-118. http://ijopaar.com/files/CurrentIssue/14A16107.pdf
9. Miyan, M., "Differential Acoustic Resonance Spectroscopy Analysis of Fluids in Porous Media", *International Journal of Pure and Applied Researches (IJOPAAR),* (2016), Volume 2(Issue 1), pp. 22-30. http://ijopaar.com/files/CurrentIssue/A16209.PDF
10. Miyan, M. and Pant, P. K., Fluid Flow through Woven Fabrics by the Lattice-Boltzmann Method, *American Journal of Engineering Research (AJER)*, (2015); 4(9):160-167; http://www.ajer.org/papers/v4(09)/W04901600167.pdf
11. Pant, P. K., "Analysis of Multiphase Flow under the Ground Water", *International Journal of Pure and Applied Researches (IJOPAAR),* (2016), Volume 1(Issue 1), pp. 09-17. http://ijopaar.com/files/CurrentIssue/A16103.pdf
12. RASI, M., et al., "Permeability of paper: Experiments and numerical simulations, in TAPPI International Paper Physics conference", TAPPI Press, Atlanta, (1999), pp. 297–306.
13. Shukla, M. K., "Propagation of Characteristic Wave Front through a Two Phase Mixture of Gas and Dust Particles", *International Journal of Pure and Applied Researches (IJOPAAR),* (2016), Volume 1(Issue 1), pp. 18-30. http://ijopaar.com/files/CurrentIssue/A16104.pdf
14. http://www.slideshare.net/MercierMercier/finale-paper-physics2007-4219791.